University of Baghdad
College of Engineering
JOURNAL OF ENGINEERING

Journal of Engineering

journal homepage: www.jcoeng.edu.iq

Volume 30 Number 8 August 2024

Ignition Delay Period Prediction for Compression Ignition Engines Fueled with Ethanol/Diesel Blends

Hemin Othman Ghareeb[1*], **Hassan Abad Al-Wahab Anjal**[2]

[1]Department of Mechanical and Mechatronics Engineering, College of Engineering, Salahaddin University, Erbil, Iraq

[2]Department of Aeronautical Engineering, College of Technical Engineering, Alkitab University, Kirkuk, Iraq

ABSTRACT

A key characteristic of diesel engines is predicting the ignition delay period. This work predicts the ignition delay in diesel engines using combinations of ethanol/diesel fuel blend and pure diesel as fuel replacements. It provides an empirical formula for predicting delay periods. A growing interest in alternative fuel blends, representing a substantial shift from the use of traditional diesel fuel, is reported. Modern study is focused on examining these combinations and how they might affect the dynamics of combustion in diesel engines. Experiments were carried out utilizing five different ethanol/diesel fuel blends, including pure diesel, with ethanol percentages varying from 5% to 20% in 5% quantities. Tests were conducted at a constant engine speed of 1,500 rpm, with various compression ratios of 16, 17, and 18, with torque levels ranging from 0 to 21 N.m. In this study, general formulas for predicting ignition delay are constructed numerically. There was a greater consistency between the experimental outcomes and the expected ignition delay. The findings indicated that the E20 combined fuel continuously exhibited the least igniting delay period across all compression ratio variables. The findings demonstrated that the ignition delay period starts to shorten with increased cetane number, ignition pressure, temperature, and equivalency ratio. A shorter period of ignition delay is the outcome of higher compression ratios. The predictive model created here is a ground-breaking addition to the industry, offering a solid foundation for assessing the efficiency and emissions properties of different ethanol/diesel blends.

Keywords: Ignition delay period, Ethanol, Equivalence ratio, Cetane number.

1. INTRODUCTION

Internal combustion engines have found widespread use across various transportation applications and serve as the main supply of energy in numerous industrial sectors. These engines are responsible for converting the potential energy contained in the fuel into kinetic

*Corresponding author
Peer review under the responsibility of University of Baghdad.
https://doi.org/10.31026/j.eng.2024.08.04

Article received: 14/10/2023
Article revised: 24/03/2024
Article accepted: 17/04/2024
Article published: 01/08/2024

energy, typically manifested as mechanical work generated through the rotation of an engine crankshaft. As explained by **(Pulkarbed, 1997)**, this energy conversion begins with transforming the chemical energy in fuel into thermal energy through processes like combustion/oxidation within the engine. Consequently, the gases within the engine experience heating, leading to elevated temperature and pressure levels. Diesel engines, a type of internal combustion engine known for their notably high compression ratios, offer a distinct advantage in terms of power generation and thermal efficiency. This characteristic makes them particularly well-suited for applications such as off-road vehicles, as noted by **(Taylor, 1985)**. In the realm of internal combustion engines, a range of alternative fuels exists, and one readily accessible option is ethanol. When blended with diesel fuel, ethanol can serve as a biodiesel, making it a convenient and accessible alternative fuel source, as highlighted by **(Wrage and Goering, 1980)**. Renewable and environmentally friendly ethanol can be used independently or in combination with other diesel fuels. The technique of converting different waste materials into biofuels, including ethanol, is examined by **(Ibrahim et al., 2017)**. The amount of ethanol obtained during fermentation was calculated using a gas chromatography instrument. It seems that, in the future, there can be a great deal of interest in producing ethanol at an extensive scale from cellulosic materials. Renewable and eco-friendly, ethanol can be consumed either by itself or in combination with additional diesel fuels. **(Selvakumar et al., 2015)** are becoming more interested in the consumption of ethanol together with diesel because of its lower risk and renewable character compared with traditional fuel. They conducted a theoretical study using CN, Cr, and T to predict ignition delay. The findings demonstrated that increased CN reduced the biodiesel's igniting delay. **(Kwanchareon et al., 2007)** consumed ethanol and combined it with diesel fuel without changing the engine. They demonstrate that ethanol's immiscibility in diesel fuel across a large temperature variation is an essential drawback of diesel fuel combinations with ethanol, which must be addressed by mixing an emulsifier and an additional solvent. The formula C_2H_5OH represents the organic chemical group that includes ethanol. It is made from oxygenated crops and gives fuel additional oxygen.

(Hansen et al., 2005) found that blending ethanol with diesel fuel reduces the number of particulate matter particles from diesel engines and increases engine performance. **(Teng et al., 2003)** carried out an empirical examination of the igniting delay of the dimethyl ether. The ignition delay was analyzed based on physical phenomena. They found that the short igniting delay is primarily due to the dimethyl ether's limited physical delay, and the dimethyl ether's quick droplet evaporate rate is primarily responsible for the uneven dimethyl ether spray boundary. Lastly, a relationship between temperature, pressure, and ignition delay was created and used to model engine combustion. **(Ghareeb and Anjal, 2023)** examined the effects of fuel combined containing ethanol and diesel on emission levels and the performance of diesel engines. Their findings demonstrate that using mixed diesel fuel with a higher ethanol portion improved performance and minimized emissions. The ignition delay period is one of the most significant aspects of the performance of a diesel engine. relies on the factors that determine when combustion starts. **(Al-Namie et al., 2012)** looked at how engines operate better and emit fewer greenhouse gases when they run on a combination of diesel and biodiesel.

(Yahuza and Dandakouta, 2015) investigate the qualities of diesel and ethanol fuel combinations that significantly impact engine performance and have positive effects on minor changes to fuel injection parameters that could lead to additional advances in emissions reduction. They demonstrated that these blends were suitable for use in modern diesel engines. Absolute ethanol blends well with diesel fuel in hot conditions. **(Saadi et al.,**

2016) examined the dependence of ignition delay on equivalency ratio and cetane number, emphasising developing empirical ignition delay models based on engine experimental results. Their findings indicate that a rise in CN, P_{ign}, and T_{ign} reduces the ignition delay period, and ethanol is one of the best options for enhancing ignition quality. Compared to diesel fuel alone, they demonstrate that E10 combined fuel has the smallest ignition delay. The combustion parameters of diesel, pure biodiesel made from Jatropha oil, and mixed with acetone and ethanol were studied by **(Gogoi et al., 2013)**. According to their investigation, biodiesel has a shorter ignition delay than ordinary diesel, indicating that ethanol is a very good option for improving fuel ignition characteristics. Their study found that 20% ethanol reduced the ignition delay compared to other diesel fuels. Ignition delay is caused by mass interchange **(Soner et al., 2016)**. The impacts of different nanoparticle/diesel fuel blends on the physical properties of the fuel were investigated to enhance its qualities and promote performance **(Altaee, 2022)**. His research indicates that increasing nanoparticle levels could make diesel fuel more fuel-efficient. Nanoparticles reduce ignition delay by altering evaporation duration. When nanoparticles are added to diesel fuel, emission levels decrease, indicating full combustion **(Ajin and Sajith, 2013).**

The duration between the onset of fuel injection and the initiation of combustion is known as the ignition delay. Two methods for estimating the ignition delay are the illumination delay and the pressure rise **(Daniel and Ademola, 2013).** An injection's pressure rise refers to the period from the time the injection is started until the pressure rise during combustion is apparent. In contrast, illumination delay is the delay between injection and illumination **(Kwon et al., 1989).** There are two main factors affecting the ignition delay period. The first set of engine design parameters includes Cr and Torque. The fuel's physical and chemical characteristics make up the second. The fuel's chemical and physical properties are covered in the second group. Chemical delay is the time that occurs following the physical delay time ends and before the fuel auto-ignites and flame come up. Physical delay is the period from when the fuel is injected until it reaches the temperature required for self-ignition when it is atomized, evaporated, and combined with air **(Hussain et al., 2013)**. Pre-flame responses occur at this time. Because the processes included are so complicated, it is quite hard to distinguish between these two delay intervals precisely **(Shahabuddin et al., 2013)**.

The combustion characteristics of rapeseed mixed with diesel fuel, ethanol, and biodiesel were studied **(Chen et al., 2014)**. Their results showed that the peak pressure during combustion stays comparatively low at low load conditions. However, adding ethanol to the blend dramatically causes the engine's combustion pressure as the engine load reaches moderate and high levels. Their tests found that adding 5% ethanol by volume improved engine performance and combustion characteristics. In a different study, **(Sahoo and Das, 2009)** examined the diesel engine fuel combustion characteristics of biodiesel made from Jatropha, Karanla, and Polanga oils.

In comparison to using only pure diesel fuel, the study's findings showed that all biodiesel fuels had higher peak pressures in the cylinder and a shorter ignition delay period. To predict the ignition delay period, this study generates empirical equations as a function of T_{ign}, P_{ign}, and Φ. Throughout the study, these variables will be affected by a range of compression ratios. The ignition delay for different blends of biodiesel made from waste oil combined with diesel fuel was predicted by **(Kasaby and Nemit, 2013)**. They found that 50% of blends had a shorter delay period than other combinations.

The focus of this study's originality is on predicting the delay periods for diesel engines running on combinations of ethanol and diesel fuel. This is an important change from using diesel fuel as is often done and opens up the option to investigate different fuel compositions. The main contributions to innovation include investigating how ethanol/diesel fuel blends affect the delay period in diesel engines, building mathematical models to estimate this delay period to improve engine performance when using alternative fuels, and advancing our understanding of combustion dynamics and behavior. The desired mathematical and experimental variables include the percentage of ethanol in the fuel blends (5% to 20% in 5% increments), the compression ratios (16, 17, and 18), the engine speed (constant at 1500 rpm), the torque levels (0 to 21 N.m.), temperature and ignition pressure, and the equivalency ratio. The study intends to provide a significant understanding of the combustibility characteristics of ethanol/diesel fuel blends and their suitability for use in diesel engines through a methodical investigation of these variables and their influence on the delay period.

2. THEORETICAL APPROACH

2.1 Modeling of Empirical Ignition Delay

To conduct the current study, the volume and pressure inside the cylinder's combustion chamber at various crank angles were measured, ranging from zero to 720^{o}. Piezoelectric pressure sensor signals were used to record the torque and compression ratio numbers data. By noting a sudden increase in cylinder pressure (also known as ignition pressure), the combustion process was evident. The start of combustion was confirmed using the logarithmic pressure-volume curve. Since the compression process in this study follows a polytropic (pv^n=constant) path, the logarithmic pressure-volume indicator diagram exhibits linearity, with the endpoint of this diagram signifying the commencement of combustion. The slope of the line is the polytropic index (n). **Figs. 1** to **3** provide visual representations of the pressure-crank angle (P-θ), volume-crank angle (V-θ) indicator diagram, and the logarithmic pressure-volume curve, respectively.
The ignition delay period is characterized as measuring the crank angle interval in degrees between the commencement of fuel injection and the initiation of combustion. In this study configuration, fuel injection is set to commence 20 degrees before reaching the top dead center. Consequently, the ignition delay period was calculated by comparing this angle with the angle at which combustion initiates.

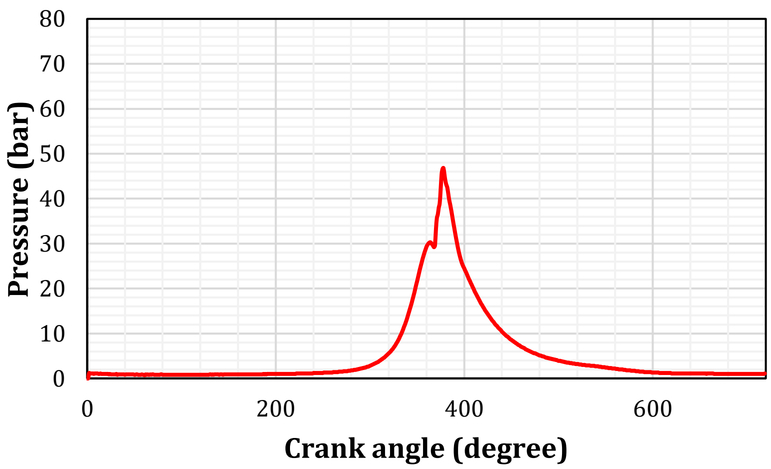

Figure 1. The pressure-crank angle (P-θ) indicator diagram.

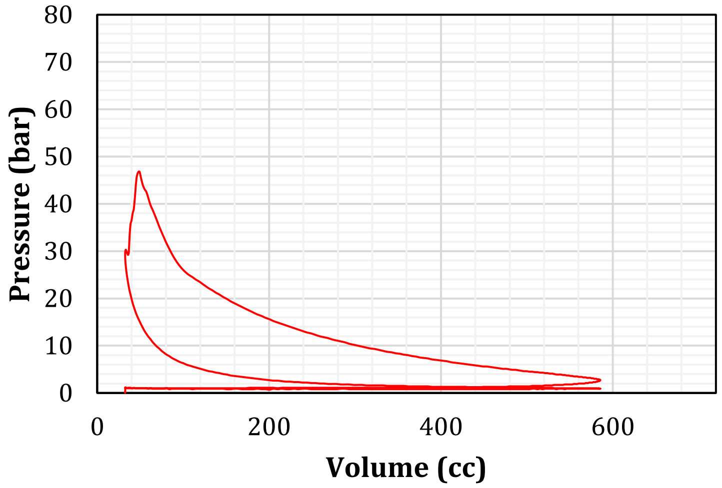

Figure 2. The volume-crank angle (V-θ) indicator diagram.

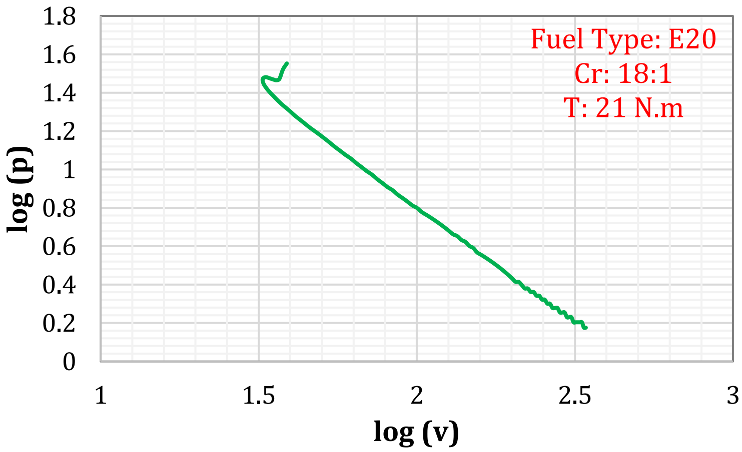

Figure 3. The logarithmic pressure-volume curve.

(Saadi et al., 2016) suggested and utilized this number while utilizing diesel and biodiesel fuel blends to accomplish the necessary engine characteristics. Numerous empirical equations have been established to predict the ignition delay period in compression ignition engines. These formulas are established based on the parameters of the engine and charge, and many of them utilize an Arrhenius formula similar to the one proposed by **(Wolfer, 1938)**. Arrhenius's formula is crucial in determining the ignition delay period, establishing a connection between this period, ignition pressure, and ignition temperature through a semi-empirical equation as depicted in Eq. (1).

$$\tau_{id} = A(P_{ign})^{-B} e^{\left(\frac{E_a}{RT_{ign}}\right)} \quad (1)$$

Eq. (1) primarily focused on describing the ignition delay period (τ_{ign}) with specific regard to pressure (P_{ign}), activation energy (E_a), gas constant (R), and temperature (T_{ign}). The Wolfers equation is a mathematical expression that establishes a relationship between the properties of a fuel and its combustion behavior. The formula's variables A, B, and E_a correspond to the characteristics of each fuel. This equation converts crank angle degrees into milliseconds by dividing by (0.006 * N). According to **(Shahrani, 2017)**, the conversion factor of 0.006 indicates how many milliseconds are required for every degree of crank angle, considering a specific engine speed and crank angle.

Eq. (2) indicates how it is proportionately inversely related to Ea and CN. CN decreases as E_a increases. Rapid ignition, shorter delay times, and improved combustion characteristics are all impacted by larger fuel CN **(Hardenberg and Hase, 1979)**.

$$E_a = \frac{618840}{CN+25} \quad (2)$$

Lower cetane numbers cause longer ignition delays, according to **(Hardenberg and Ehnert, 1981)**, giving fuel more time to vaporize before combustion begins.
The most commonly utilized empirical formula for estimating ignition delay in diesel engines was developed by **(Stringer, et al., 1970)** and is as follows:

$$\tau_{id} = 0.0405(P_{ign})^{-0.757} e^{(\frac{5473}{T_{ign}})} \quad (3)$$

Empirical equations for computing ignition delay can be constructed by employing variables including P_{ign} and T_{ign}. The ignition delay can be predicted with these practical and helpful equations. Nevertheless, the amount and quality of the data used to generate these equations will determine their accuracy. The temperature at the ignition point is calculated by plugging in the given values of Ti-1, Pi, and Pi-1 into Eq. (4) and utilizing a MATLAB code. This equation considers the correlation between temperature and pressure during the compression process while assuming polytropic compression characteristics. The MATLAB code facilitates the calculation process, providing the desired temperature value at the ignition point.

$$T_i = T_{i-1}(\frac{P_i}{P_{i-1}})^{(\frac{n-1}{n})} \quad (4)$$

Using pressure and volume data, Eq. (5) can be applied to determine the polytropic compression constant (n) for different ethanol/diesel fuel blends under varying torque and compression ratio conditions.

$$V_i = V_{i-1}(\frac{P_{i-1}}{P_i})^{(\frac{1}{n})} \quad (5)$$

2.2 Air-fuel ratio (A/F) and Equivalence ratio (Φ)

Air-fuel ratios are expressed as the volume ratio of air to fuel in a fuel-air mixture for complete combustion. Equivalence ratios compare actual A/F to stoichiometric A/F. Stoichiometric mixtures consist of 1 equivalence ratio, while fuel-lean mixtures consist of values below 1, and fuel-rich mixtures consist of values above 1. As part of engine testing, ethanol/diesel blends and pure diesel fuel alone are analyzed to determine the air-fuel ratio. In engine operation, this method provides accurate information on the composition of the A/F mixture.
In contrast, the stoichiometric A/F is calculated by assuming stoichiometric combustion for specific blends of ethanol and diesel. The stoichiometry and chemical composition of the fuel are considered when performing this calculation. The stoichiometric combustion equations for various fuel scenarios, including pure diesel fuel (E0) and ethanol/diesel fuel blends (E5, E10, E15, E20), along with the calculation of stoichiometric air-fuel ratios, can be found in Appendix A.

3. EXPERIMENTAL WORK

3.1 Model for Engine Testing

This study selected a vertical, single-cylinder diesel engine with a four-stroke cycle, direct injection, water cooling, and a variable compression ratio mechanism as the test rig. An eddy current dynamometer, a single-cylinder diesel engine, and a data collection device comprise the major parts of the test setup. The above components work together to provide a crank angle diagram that can measure various engine performance characteristics, such as the variation in pressure and volume. To obtain the cylinder pressure values and cylinder volume as a function of crank angle, data is collected via a piezoelectric pressure transducer sensor. Subsequently, the recorded data from the test rig can be analyzed using the computer program "Engine VCR". This software facilitates the graphical and tabular representation of the data, enhancing its comprehensibility. The engine was started with diesel fuel and allowed to heat up and achieve room temperature before being started. The engine was first tested using E0 diesel fuel, and the results were reported. This process is repeated for various ethanol/diesel fuel combinations under comparable operational conditions. Assessments of combustion and steady-state performance were taken with the engine running at a constant 1500 rpm. Then, the mean of the collected data is used to perform more calculations. A useful approach to presenting the engine specifications is summarising them in **Table 1**.

Table 1. Specifications of the diesel engine test rig.

Parameter	Specifications
Type	Four Stroke, direct-injection
Max. Engine power	3.3 kW
Engine speed (N)	1500 RPM
Max. torque	21 N.m
Fuel Type	Diesel
No. of Cylinder	1
Bore	0.08 m
Length of Stroke	0.11 m
Cr Range	16:1 - 18:1
Length of Connecting road	0.23 m

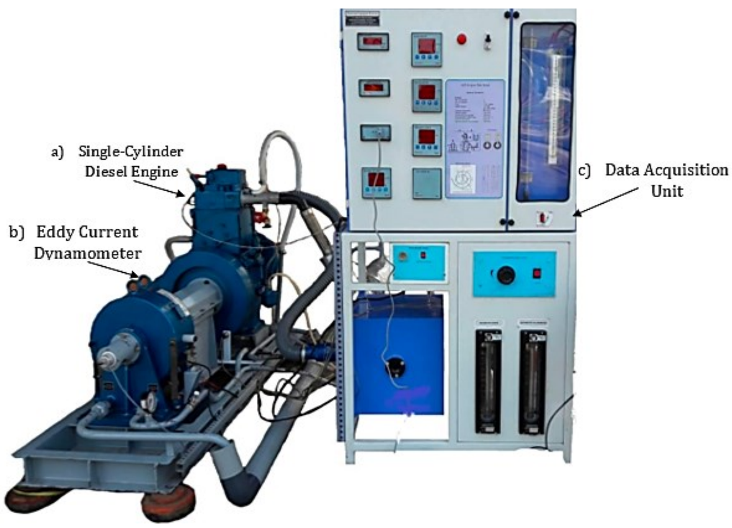

Figure 4. Configuration of the Experimental Setup for the Diesel Engine.

This tabular format aids in organizing the information and allows readers to comprehend and compare different engine specifications easily. Furthermore, **Fig. 4** is an illustrative tool for depicting the experimental setup. **Fig. 5** depicts a schematic representation of this testing apparatus.

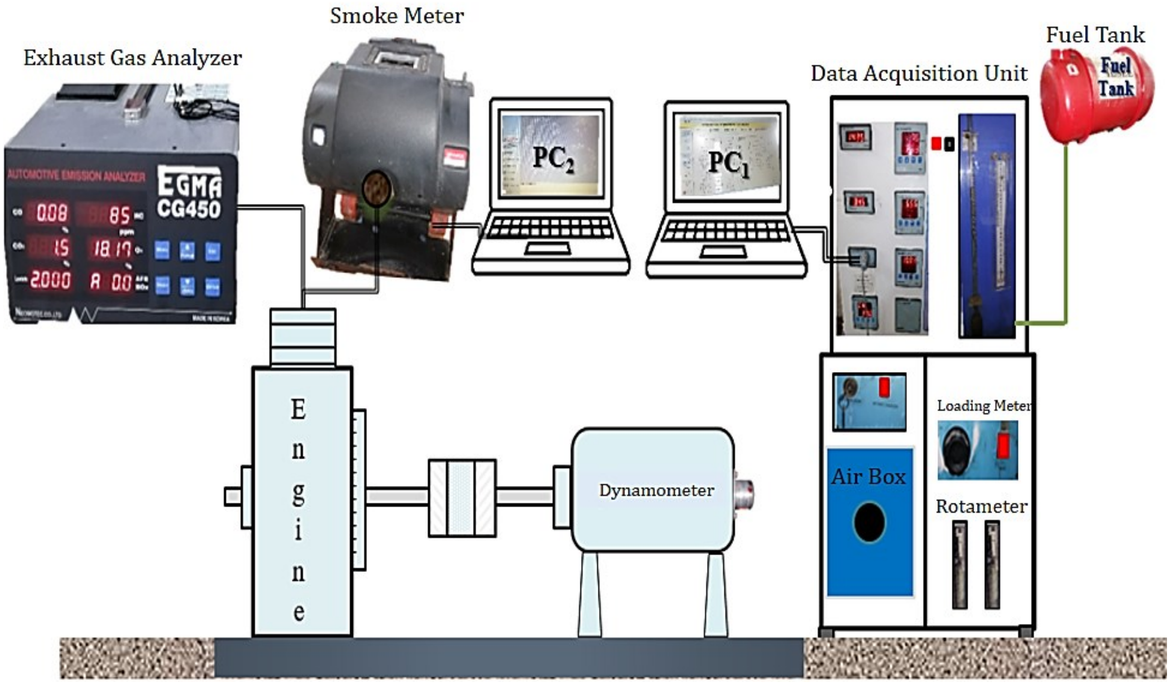

Figure 5. Schematic Diagram of the Diesel Engine Measurement System

3.2 Variety of Tested Fuels

Ethanol/diesel fuel blends were employed as the constituent materials for creating the fuel blends. The diesel fuel was sourced exclusively from the Bazian oil refinery with a chemical composition of $C_{16}H_{32}$ and a cetane number 47.6. The composition was typical of heavy diesel fuel. Gas Chromatography-Mass Spectrometry, a sophisticated analytical technique known for its accuracy in identifying and measuring chemical components in complex mixtures, was employed to ascertain this diesel fuel's chemical composition precisely. Light diesel fuel, being less dense and more volatile, contrasts with heavier diesel fuel.

Conversely, heavy diesel fuel, with its higher molecular weight and density, tends to exhibit greater stability and energy content. However, the absolute ethanol was acquired from a chemical supply store. This study examined five distinct ethanol/diesel fuel blends, including one comprising solely diesel fuel and the remaining blends combining varying proportions of ethanol with diesel fuel. The identification numbers for the test fuels are E0, E5, E10, E15, and E20. E0 is 100% pure diesel fuel, E5 is 5% ethanol and 95% diesel fuel, E10 is 10% ethanol and 90% diesel fuel, E15 is 15% ethanol and 85% diesel fuel, and E20 is 20% ethanol and 80% diesel fuel. These fuels are tested at five distinct torque values (0, 6, 11, 16, and 21 N.m.) and with three distinct compression ratios (16, 17, and 18).

Detailed fuel chemistry investigations were carried out by Sulaimani City's quality control center and nearby companies starting the engine tests. **Table 2** presents the outcomes of the chemical analysis conducted on all fuel kinds under examination. The properties of standalone diesel and blend fuels were evaluated per ASTM standards.

Table 2. The properties of ethanol/diesel fuel blend and diesel alone

Properties	E0	E5	E10	E15	E20	ASTM
Density @15°C (g/cm³)	0.827	0.8255	0.8236	0.8219	0.8195	D4052
CN	47.6	47.9	49.1	51.3	52.3	D613
Flashpoint (°C)	56.7	58.8	54.7	57.3	56.7	D56
Viscosity @ 40C°	1.8	1.78	1.94	2.1	1.77	D445
Calorific value (MJ/kg)	45.9	45.92	45.95	45.97	46.01	D4809

4. RESULTS AND DISCUSSION

4.1 Variation in-cylinder Pressure within the Combustion Chamber

When fuel burns during combustion, the pressure inside the chamber is directly proportional to that rate. Higher pressure levels are associated with faster heat release and more effective combustion. **Fig. 6** shows the cylinder pressure of several combinations of ethanol diesel fuel and pure diesel at various crank angle positions when the engine operates at maximum torque and with varied compression ratios. The results show that the cylinder pressure rises gradually until reaching peak pressure. During this period, the cylinder pressure decreases as the crank angle increases. It was observed that the top dead center is not far from where the highest pressure occurs. Additionally, for a 16 CR, peak pressures of 38.7, 39.3, 39.5, 38.7, and 41.2 bar are obtained at 17°, 19°, 20°, 21°, and 22° crank angles after TDC with E0, E5, E10, E15, and E20, respectively. Similarly, for a 17 CR, peak pressures of 39.1, 41.5, 41.6, 41.9, and 42.1 bar are achieved at 21°, 17°, 18°, 19°, and 21° crank angles after TDC with E0, E5, E10, E15, and E20, respectively. Lastly, for an 18 CR, peak pressures of 44, 45.9, 46.3, 46.5, and 46.8 bar are obtained at 15°, 16°, 15°, 16°, and 18° crank angles after TDC with E0, E5, E10, E15, and E20, respectively. When utilizing E20 ethanol/diesel fuel, the engine's measured cylinder pressure was a bit greater than when using E0 diesel fuel. The larger calorific value may be the cause of this increase in cylinder pressure, as proposed by **(Navindgi et al., 2012)**.

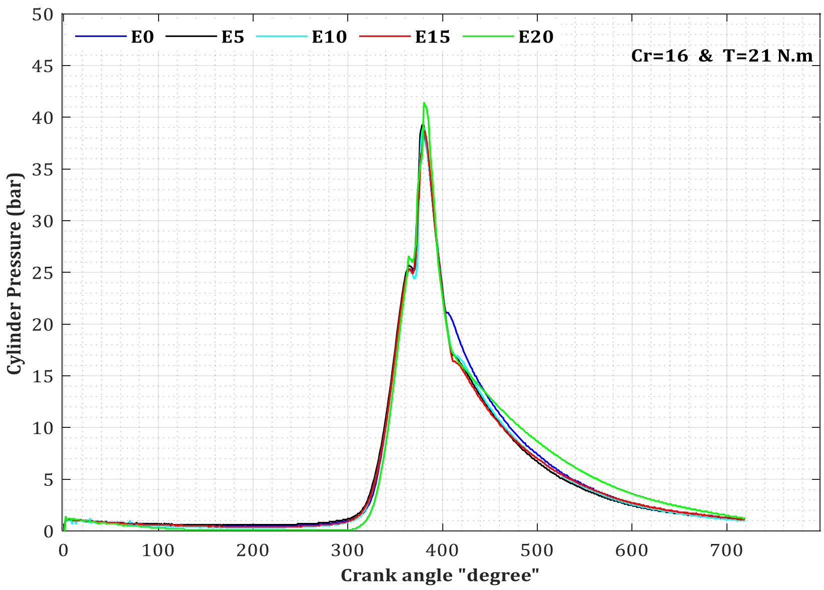

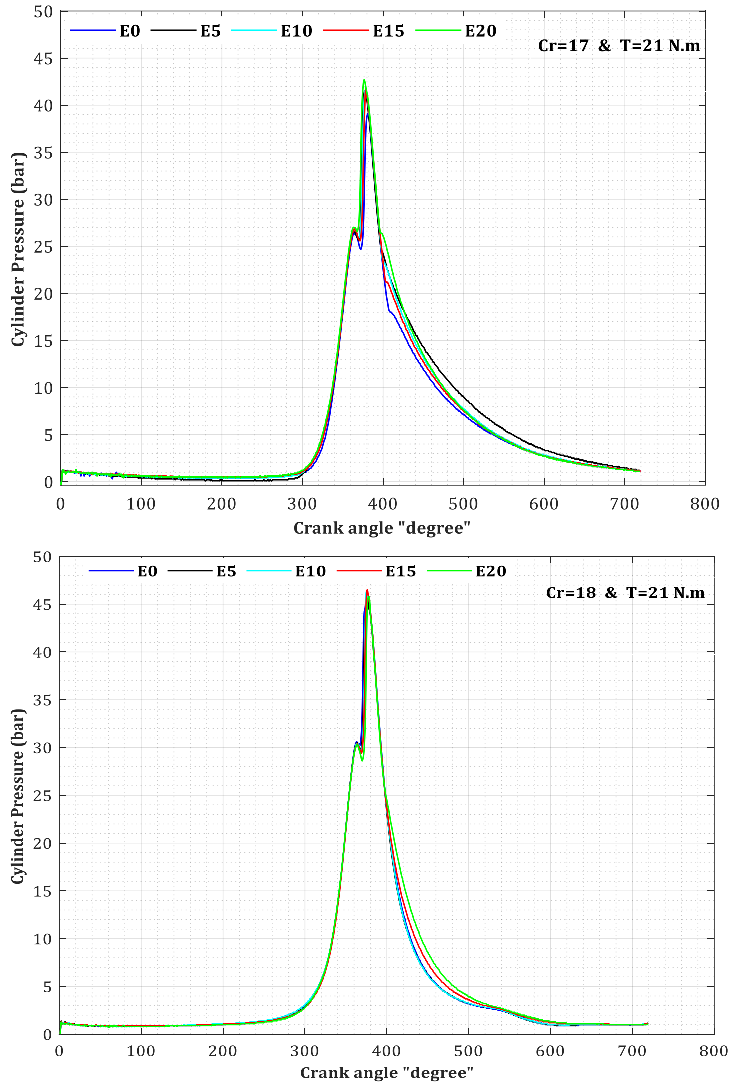

Figure 6. Cylinder Pressure Vs. Crank Angle at Different Compression Ratios and Maximum Torque (T=21 N.m) for Pure Diesel Fuel and Ethanol/Diesel Blends.

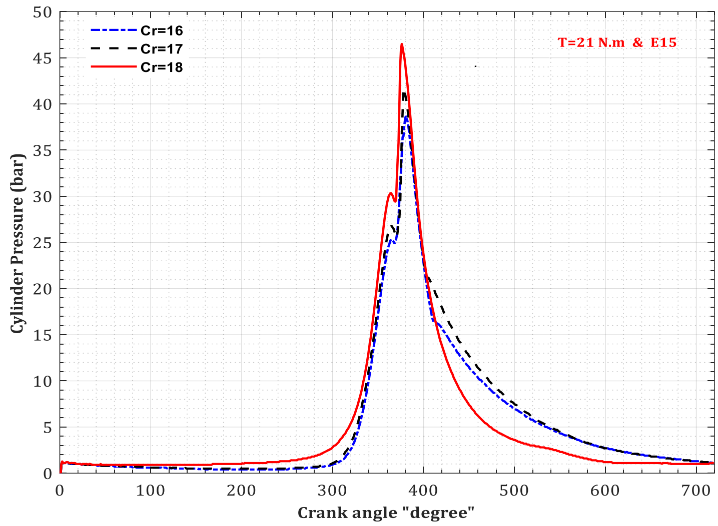

Figure 7. Effect of Compression Ratios on Cylinder Pressure and Maximum Torque with E15 Diesel Blend.

There is no virtual difference in the cylinder pressure variations between pure diesel and ethanol/diesel fuel blends until the compression ratio approaches its maximum of 18. For a given 15% ethanol (E15) diesel fuel blend, **Fig. 7** shows the relationship between the variance in the cylinder pressure and crank angle for a range of compression ratios at the optimum torque. One possible explanation for this trend is that when the compression ratio increases, the fuel-air mixture gets denser, which makes it easier for burnt and unburned components to combine more effectively. Studies by (**Huang et al., 2007**) and (**Zheng et al., 2009**) are consistent with this point of view. Higher compression ratios resulted in higher cylinder pressure, according to a study (**Datta and Kumar, 2016**).

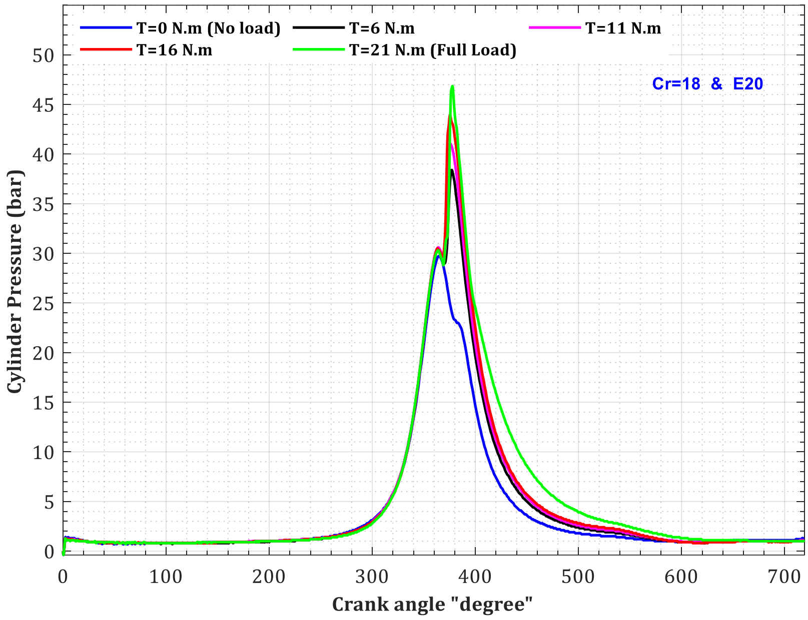

Figure 8. Analyzing Cylinder Pressure Fluctuations in E20 Ethanol/Diesel Blend at Different Torque Levels.

When employing an 18 compression ratio and type of E20 ethanol/diesel fuel blend, the relationship between crank angle and cylinder pressure is shown in **Fig. 8.** The figure shows that the variation in cylinder pressure increases as torque increases. Reduced values for cylinder pressure indicate an inefficient engine, meaning that less work is done during combustion. According to a report by **(Ghareeb and Anjal, 2023)**, lower cylinder pressure can also lead to incomplete combustion, increased emissions, and an overall reduction in engine performance.

A diesel engine's increased fuel injection volume is the main reason for the larger peak cylinder pressure at higher torque levels. More diesel fuel is in the combustion chamber due to the higher fuel injection rate. Because of the high pressure and temperature, this diesel fuel spontaneously ignites when injected into the hot, compressed air. This quick and intense combustion creates High peak pressures inside the combustion chamber.

4.2 Effect of Ethanol/Diesel Fuel Blends on Ignition Delay Period

This study introduces new parameters, namely ignition pressure, ignition temperature, and equivalence ratio, which can be utilized to develop empirical equations for ignition delay. The study includes a specific case employed to determine empirical formulas for the ignition delay period. **(Bahnasy and Kotb, 1994)** proposed a modification of the Arrhenius equation to predict the ignition delay for diesel fuels while considering biodiesel, in agreement with **(Heywood, 1988)**. The parameters included in this modification are Φ, T_{ign}, and P_{ign}. Eq. (6), which takes a non-linear form based on the Arrhenius equation, is shown below.

$$\tau_{id} = A(P_{ign})^{-B}(\emptyset)^{-C}e^{(\frac{E_a}{RT_{ign}})} \quad (6)$$

According to this updated equation, the ignition temperature, activation energy, equivalency ratio, ignition pressure, and parameters A, B, and C affect the ignition delay. Usually, the least square fitting method is used to identify the exact values of A, B, and C. Eq. (7) is obtained by taking the logarithm of both sides of Eq. (6):

$$\ln(\tau) = \ln(A) - B\ln\left(P_{ign}\right) - \mathrm{C}\ln(\emptyset) + \frac{E_a}{RT_{ign}} \quad (7)$$

When programming languages are used, solving Eq. (7) is simple. Under various torque options, equations were created for pure diesel fuel and ethanol/diesel fuel blend. The ignition delay as a function of all parameters (P, T, Φ) can be expressed by the following general empirical equations:

When T=0 N.m

For **E0** $\tau_{id} = 3.4744 * 10^9(P_{ign})^{3.9846}(\emptyset)^{15.2308}e^{(\frac{1025.2}{T_{ign}})}$ (8)

For **E5** $\tau_{id} = 6.4866 * 10^{-4}(P_{ign})^{-1.8458}(\emptyset)^{25.4206}e^{(\frac{1021.8}{T_{ign}})}$ (9)

For **E10** $\tau_{id} = 5.1422\,(P_{ign})^{-1.762}(\emptyset)^{5.7893}e^{(\frac{1004.5}{T_{ign}})}$ (10)

For **E15** $\tau_{id} = 6.03 * 10^7(P_{ign})^{-5.7809}(\emptyset)^{-5.1875}e^{(\frac{975.5}{T_{ign}})}$ (11)

For **E20** $\tau_{id} = 7.81 * 10^{-8}(P_{ign})^{3.0502}(\emptyset)^{14.7111}e^{(\frac{962.8}{T_{ign}})}$ (12)

When T=6 N.m

For **E0** $\tau_{id} = 1.1187\,(P_{ign})^{-1.0972}(\emptyset)^{5.4184}e^{(\frac{1025.2}{T_{ign}})}$ (13)

For **E5** $\tau_{id} = 0.6973\,(P_{ign})^{-0.1867}(\emptyset)^{-3.415}\,e^{(\frac{1021.8}{T_{ign}})}$ (14)

For **E10** $\tau_{id} = 15.1064\,(P_{ign})^{-1.5187}(\emptyset)^{1.6633}\,e^{(\frac{1004.5}{T_{ign}})}$ (15)

For **E15** $\tau_{id} = 45.706\,(P_{ign})^{-1.6977}(\emptyset)^{-0.2719}e^{(\frac{975.5}{T_{ign}})}$ (16)

For **E20** $\tau_{id} = 138.5037\,(P_{ign})^{-2.2426}(\emptyset)^{0.0073}\,e^{(\frac{962.8}{T_{ign}})}$ (17)

When T=11 N.m

For **E0** $\tau_{id} = 0.2867\,(P_{ign})^{1.3138}(\emptyset)^{-7.7019}\,e^{(\frac{1025.2}{T_{ign}})}$ (18)

For **E5** $\tau_{id} = 89.5632(P_{ign})^{-1.4414}(\emptyset)^{2.3517}\,e^{(\frac{1021.8}{T_{ign}})}$ (19)

For **E10** $\tau_{id} = 130.088\,(P_{ign})^{-1.5518}(\emptyset)^{2.2001}\,e^{(\frac{1004.5}{T_{ign}})}$ (20)

For **E15** $\tau_{id} = 0.3045\,(P_{ign})^{0.3876}(\emptyset)^{0.6819}\,e^{(\frac{975.5}{T_{ign}})}$ (21)

For **E20** $\tau_{id} = 1.7166\,(P_{ign})^{-0.1563}(\emptyset)^{0.96}\,e^{(\frac{962.8}{T_{ign}})}$ (22)

When T=16 N.m

For **E0** $\tau_{id} = 0.3038\,(P_{ign})^{0.6515}(\emptyset)^{-2.7693}\,e^{(\frac{1025.2}{T_{ign}})}$ (23)

For **E5** $\tau_{id} = 1.9052(P_{ign})^{-0.2305}(\emptyset)^{1.35}\,e^{(\frac{1021.8}{T_{ign}})}$ (24)

For **E10** $\tau_{id} = 0.1078\,(P_{ign})^{0.6295}(\emptyset)^{1.1794}\,e^{(\frac{1004.5}{T_{ign}})}$ (25)

For **E15** $\tau_{id} = 0.5698\,(P_{ign})^{0.1755}(\emptyset)^{0.4595}\,e^{(\frac{975.5}{T_{ign}})}$ (26)

For **E20** $\tau_{id} = 1.4422\,(P_{ign})^{-0.0901}(\emptyset)^{0.462}\,e^{(\frac{962.8}{T_{ign}})}$ (27)

When T=21 N.m

For **E0** $\tau_{id} = 2.7632\,(P_{ign})^{-0.2318}(\emptyset)^{0.15618}\,e^{(\frac{1025.2}{T_{ign}})}$ (28)

For **E5** $\tau_{id} = 0.3712(P_{ign})^{0.2872}(\emptyset)^{0.7964}\,e^{(\frac{1021.8}{T_{ign}})}$ (29)

For **E10** $\tau_{id} = 116.07\,(P_{ign})^{-1.2527}(\emptyset)^{-1.0241}\,e^{(\frac{1004.5}{T_{ign}})}$ (30)

For **E15** $\tau_{id} = 26.373\,(P_{ign})^{-0.796}(\emptyset)^{-3.379}\,e^{(\frac{975.5}{T_{ign}})}$ (31)

For **E20** $\tau_{id} = 1.33 * 10^{8}(P_{ign})^{5.3286}(\emptyset)^{-1.5317}\,e^{(\frac{962.8}{T_{ign}})}$ (32)

Eq. (2) is used to calculate the apparent activation energy. **Table 3** contains the values of CN, E_a, and E_a/R for pure diesel and ethanol/diesel fuel blend. Remarkably, the apparent activation energy decreases as the fuel's cetane number rises.

Table 3. Cetane Number Measurement and Apparent Activation Energy Calculation for Ethanol/Diesel Fuel Blends and Pure Diesel

Type of Fuel	CN	E_a	Ea /R (K)
E0	47.6	8523.967	1025.2
E5	47.9	8488.889	1021
E10	49.1	8351.417	1004.5
E15	51.3	8110.616	975.5
E20	52.3	8005.692	962.8

The predicted ignition delay period for various torque levels over a range of compression ratios was obtained by entering the P_{ign}, T_{ign}, and Φ values into the empirical formulae. **Fig.9** provides a graphic representation of these predicted values. This figure shows that the original diesel fuel has an experimental ignition delay of 2 ms at 16 Cr. In contrast, the ethanol/diesel fuel blended at E5, E10, E15, and E20 is 1.78 ms, 1.67 ms, 1.45 ms, and 1.4 ms, respectively. Similarly, the E0 fuel has an experimental ignition delay of 1.67 ms at 18 Cr, whereas the blended at E5, E10, E15, and E20 is 1.45 ms, 1.12 ms, 0.9 ms, and 0.7 ms, respectively. This indicates that the ignition delay for 16 Cr is more significant than that of 18 Cr. The overall difference is around 3% between the measured and predicted ignition delays. An interesting tendency noted is that all ethanol/diesel fuel blends decrease as the

Cr increases. This outcome is more in line with research findings from studies **(Shahrani, 2017; Mustafa et al., 2008)**.

Higher compression ratios allow the pressure inside the combustion chamber to rise, accelerating the ignition and burning of the fuel and air combination. Thus, shorter ignition delays are produced by higher compression ratios. The study's predictive models accurately predict ignition delay across various scenarios, as evidenced by the close correlation between predicted and experimental results. This uniformity shows that our outcome models are a dependable resource for investigating and grading combustion processes. In addition, the figure indicates that the value of the ignition delay period in the kind E20 of ethanol/diesel fuel blend seems to be shorter than in diesel alone. According to the study, diesel appears to ignite more slowly than biodiesel **(Sahoo et al., 2005)**. Because of these differences in molecular shape and CN, diesel and ethanol fuel combined possess various chemical compositions and igniting properties. Greater compression ratios accelerate chemical reactions and autoignition by raising the temperature and pressure inside the engine's combustion chamber. By encouraging cold conditions processes, ethanol in the fuel blend modified the ignition chemistry and affected the time required for ignition in high-pressure and high-temperature situations.

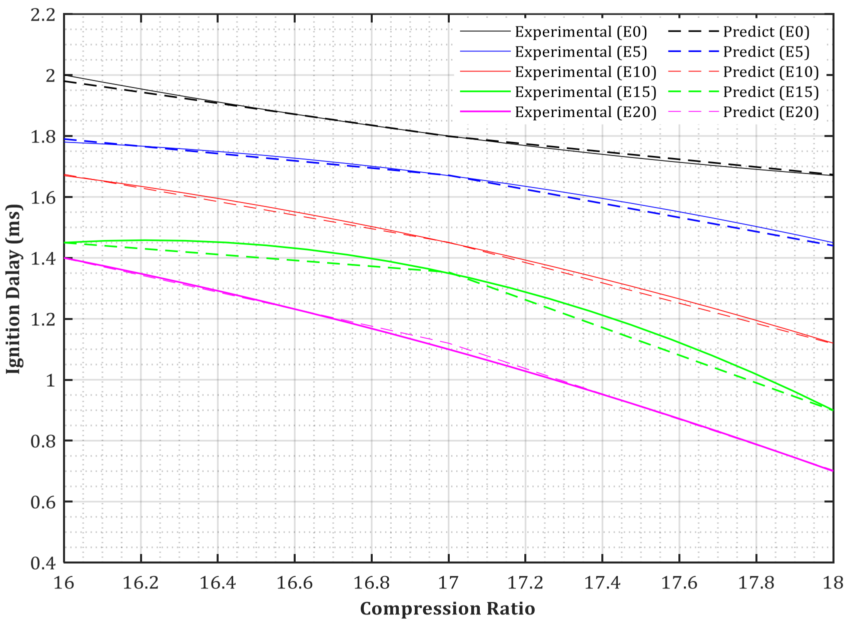

Figure 9. Ignition Delay Versus Compression Ratio for Pure Diesel and Ethanol/Diesel Blend: Experimental and Predicted Data at Zero Torque.

The relationship between compression ratio and ignition delay period at a constant 6 N.m. torque for pure diesel and ethanol/diesel fuel blends is shown in **Fig. 10**. For all ethanol/diesel fuel blends. A consistent pattern shows that the ignition delay period decreases with increasing compression ratio. The total reduction in predicted ignition delay from Cr=16 to Cr=18 was calculated to be 13.1%, 15.1%, 16.4%, 18.6%, and 22% for E0, E5, E10, E15, and E20, respectively. The total reduction in measured ignition delay was calculated to be 13.4%, 15.3%, 16.5%, 18.7%, and 22.1% for E0, E5, E10, E15, and E20, respectively.

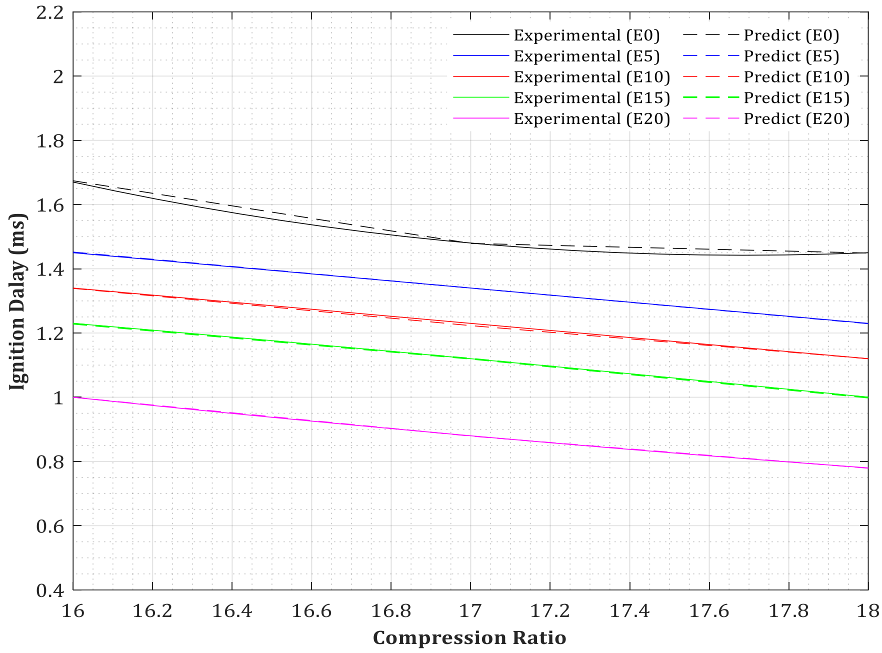

Figure 10. Ignition Delay Versus Compression Ratio for Pure Diesel and Ethanol/Diesel Blend: Experimental and Predicted Data at Six Torque.

There is more convergence between the measured and predicted ignition delays, as evidenced by the 1.2% total deviation between them. 1.2% variation could be considered impressive and suitable. Compared to **Fig. 9**, the ignition delay period decreases as torque levels increase from 0 to 6 N.m. This initial decrease is explained by the procedure used in this study, which uses an unexpected pressure rise in the pressure-crank angle diagram to indicate ignition initiation.

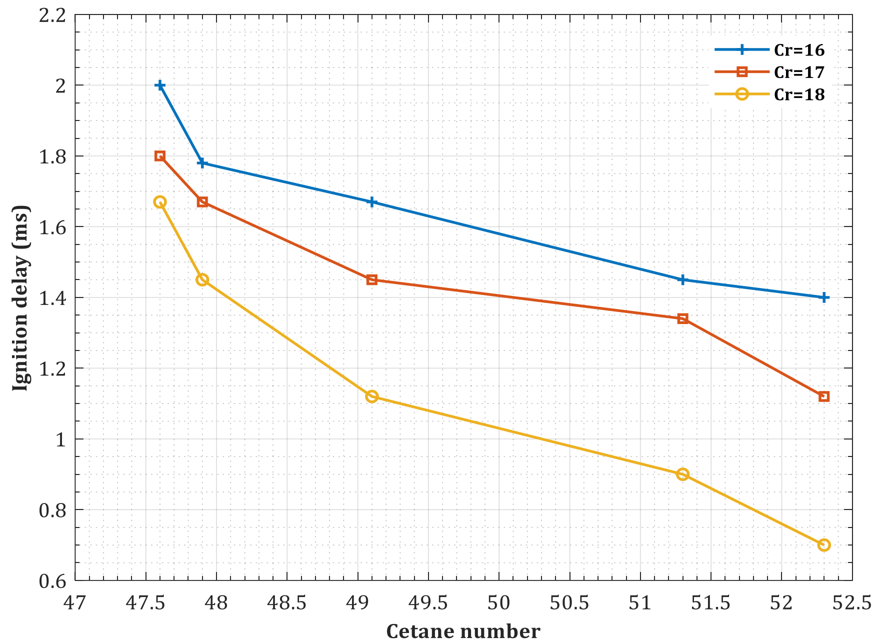

Figure 11. Effect of Cetane Number on Ignition Delay Period at Zero Torque for Different Compression Ratios.

Fig.11 illustrates how the ignition delay period is affected by the cetane number at various compression ratios. With increasing CN, ignition delay decreases. For compression ratios 16,17,18, ignition delay decreases by 30 %, 37.7 %, and 58 %. In the case of CN=47.6, there is a 10 % total deviation in ignition delay between 16 and 17 Cr and a 7.2 % total deviation between 17 and 18 Cr. When CN approaches 52.3, the deviation increases by approximately 20% and 32%. There may be changes in combustion dynamics in major operating situations, as evidenced by the increase in variance when the cetane number and compression ratio near higher ranges. There may be a greater variation in ignition delay at extremely high compression ratios and cetane numbers because the combustion mechanism is more affected by turbulence, temperature variations, and fuel-air blending. A discernible decrease in the ignition delay period is correlated with a higher cetane number. The phenomenon is attributed to the reduced temperature of self-ignition, which is a crucial element accountable for the chemical lag in ignition. The relationship between the predicted ignition delay period and several variables, including ignition pressure, temperature, and equivalency ratio under various conditions, is shown in **Fig. 12**. The graph's data points, which are identified as E0, E5, E10, E15, and E20, relate to different situations. The figure shows how the ignition delay period decreases when Pign, Tign, and Φ increase for pure diesel fuel and ethanol/diesel fuel blends. This can be clarified through the combustion mixture's molecules being closer to one another due to the increased pressure. This increased closeness greatly increases the probability of regular and vigorous collisions between these molecules. This increase in collision frequency accelerates the combustion process by fostering stronger chemical reactions inside the mixture. As a result, the ignition delay period decreases with increasing pressure because combustion occurs faster. Increasing temperatures create a molecular structure that is more energetic, accelerating the kinetics of combustion and reducing the ignition delay period. The equivalency ratio in this study, which varied from 1.7 to 1, suggests that the studies were carried out in either slightly rich or rich combinations. The equivalency ratio directly impacts ignition delay. A slightly rich mixture falls in the center, producing an insignificant ignition delay. In contrast, a rich mixture, defined by an abundance of fuel, results in a shorter ignition delay. The result implies that shorter ignition delay periods were predicted compared to lean blends.

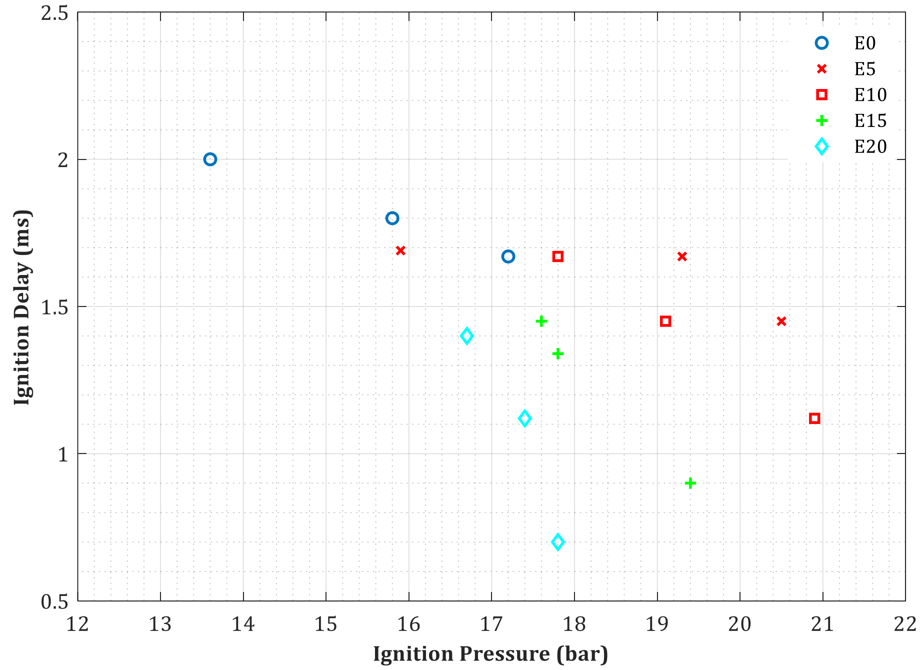

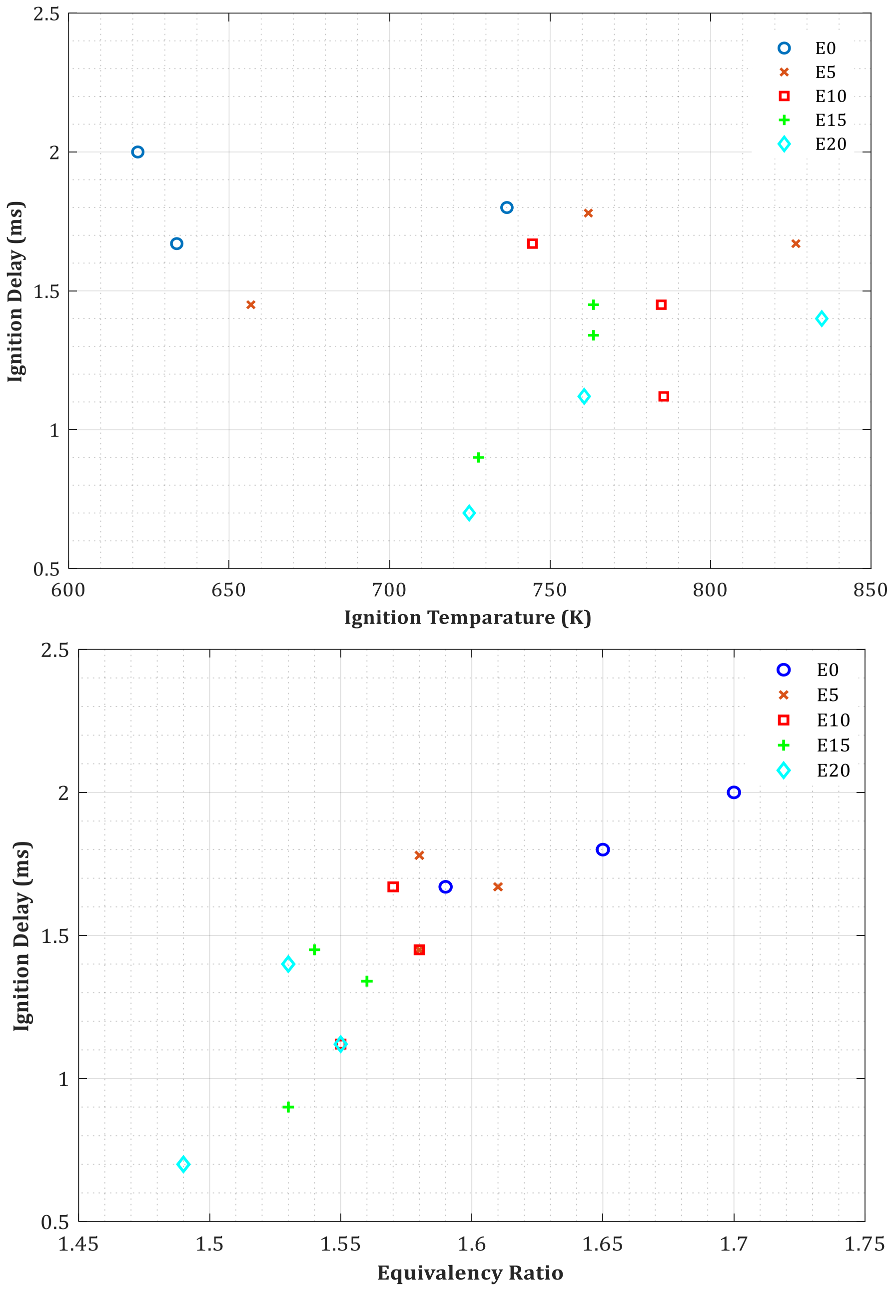

Figure 12. The Relationship Between Ignition Delay Period and Ignition Pressure, Temperature, and Equivalence Ratio for Ethanol/Diesel Blends and Pure Diesel.

Utilizing empirical equations to predict the ignition delay for the type E20 of ethanol/diesel fuel blend and pure diesel alone, as shown in **Table 4**; the outcomes were compared with findings from several other studies, such as those conducted by **(Assanis et al., 2003)**, **(Rodriguez et al., 2011; Kasaby and Nemit, 2013; Watson et al., 1980).** Although the results proposed by the first three studies and our predicted results are slightly close together, it is important to note that the fourth study's correlation slightly deviates from our expectations because Watson et al.'s correlation only uses Pign and Tign for estimating ignition delay values; it ignores Φ. There is unquestionably a far higher degree of similarities between the study's findings on the ignition delay values obtained from the empirical equations. This demonstrates the accuracy and reliability of the models used in this study.

Table 4. Comparative Analysis of Predicted Ignition Delay Periods Using Various Empirical Equation Correlations by Different Authors for E0 and E20.

Type of fuel	P_{ign}	T_{ign}	Φ	τ_{id}	**(Assanis et al., 2003)**	**(Kasaby and Nemit, 2013)**	**(Rodriguez et al., 2011)**	**(Watson et al., 1980)**
	(bar)	(K)	-	(ms)	(ms)	(ms)	(ms)	(ms)
E0	15.8	736.5	1.65	1.8	2	1.9	1.83	3.3
E20	17.4	760.6	1.55	1.72	1.8	1.75	1.7	2.9

5. CONCLUSIONS

This study was carried out to assess the impact of varying percentages of diesel fuel combined with ethanol on a single-cylinder direct-injection diesel engine. The creation of mathematical ignition delay formulas using engine test results was the main goal of this investigation. It also examined how ignition delay depended on CN, Φ, and Cr. The engine torque ranged from 0 to 21 N.m., and the engine speed was maintained at 1500 rpm throughout the testing procedure.

The study outcomes are as follows:

1. The type of ethanol (20%) blended with 80% of the diesel fuel ignites more quickly than diesel fuel alone.
2. Lower ignition delay is the result of higher compression ratios.
3. The models' accuracy and dependability are evidenced by the greater agreement between the study's conclusions and those of many other studies.
4. Shorter ignition delays result from diesel fuel's increased cetane number.
5. There is a higher agreement between practical data and the theoretical formulae for the ignition delay.

Four various ethanol/diesel fuel blends were assessed against diesel fuel alone to predict the delay period in a diesel engine. Our suggestion for further study based on the findings of this study can help develop a deeper understanding of the implications of using these blends, like the impact on engine wear and durability. Longer testing times allow for evaluating blends' effects over time on engine components, providing important information on the fuel compositions' long-term viability.

NOMENCLATURE

Symbol	Description	Symbol	Description
N	Engine Speed (rpm)	E	Ethanol
R	Gas constant, kJ/kg K	TDC	Top dead center
T	Torque, N.m	Max.	Maximum
Cr	Compression ratio, dimensionless.	T_{ign}	Ignition temperature, K.
E_a	Activation energy, J/mol	P_{ign}	Ignition pressure, bar.
CN	Cetane number, dimensionless.	τ_{id}	Ignition delay period, ms
A,B,C	Constant	Φ	Equivalence ratio, dimensionless.

Acknowledgements

The Authors extend appreciation to the Ministry of Higher Education for its financial assistance, as well as to the University of Salahadin-Erbil. The Authors are thankful for the support received from the Dean's Office of the College of Engineering and the head of the Mechanical and Mechatronics Engineering Department throughout this endeavor.

Credit Authorship Contribution Statement

Hemin Othman: Conceptualization, Investigation, Review & editing Methodology, Software, Validation. Hassan Anjal: Review & editing.

Declaration of Competing Interest

The authors declare that they have no known competing financial interests or personal relationships that could have appeared to influence the work reported in this paper.

REFERENCES

Ajin, C., S., and Sajith, V., 2013. Diesel engine emission reduction using catalytic nanoparticles: an experimental investigation. *Journal of Engineering*, 2013(1), pp. 9-13. https://doi.org/10.1155/2013/589382

Al-Namie, I., Mashkour, M. A., and Hameed, A. S., 2012. Study the effect of ceramic coating on the performance and emissions of diesel engine, *Journal of Engineering*, 18(08), pp. 935–942. https://doi.org/10.31026/j.eng.2012.08.07

Altaee, T. M., 2022. Improvement of diesel fuel engine performance by nanoparticles additives, *Journal of Engineering*, 28(4), pp. 77–90. https://doi.org/10.31026/j.eng.2022.04.06

Chen H., Yang L., Li Y., Ma Y., Zhang P., and Li J., 2014. Combustion and emission characteristics of CI engine fueled with rapeseed biodiesel, diesel and ethanol blend, *International Energy Journal*, 14, pp. 75-86.

Assanis, D.N., Filipi, Z.S., Fiveland, S.B., and Simiris, M.,2003. A predictive ignition delay correlation under steady state and transient operation of a direct injection diesel engine, *journal engineering gas turbine power*, 125, pp. 450-7. https://doi.org/10.1115/1.1563238

Bahnasy, S.H.M., and Kotb, M. M.,1994. Shock tube study for the measurement of ignition delay period of 1,2-epoxy propane n-Hexane, *The International Conference in Fuel Atomization and Spray Systems,* ICLASS-94, Ruene, France. https://doi.org/10.3390/fire6110435

Daniel C.U., and Ademola A. D., 2013. Combustion enhancers in diesel engines: magnetic field option, *Journal of Mechanical and Civil Engineering*, 5 (5), pp. 21-24. https://doi.org/10.9790/1684-0552124

Datta, A., and Kumar, B. M., 2016. Effect of compression ratio on the performance, combustion and emission from a diesel engine using palm biodiesel, *AIP Conf. Proc*. https://doi.org/10.1063/1.4958396

Gogoi, T.k., Sarma, A.K., Misra, P.S., and Syed, T. H., 2013. Combustion analysis of jatropha mrethyl estr and its ethanol and acetone blends in a diesel engine, *International Journal of Emerging Technology and Advanced Engineering*, 3 (3), pp. 51-57.

Ghareeb, H.O., and Anjal, H.A.A.W., 2023. An investigation of the impacts of ethanol-diesel blends on emission and combustion parameters of diesel engine. *International Journal of Heat & Technology*, *41*(3). pp. 513-528. https://doi.org/10.18280/ijht.410304

Hardenberg, H.O., and Hase, F.W., 1979. An empirical formula for computing the pressure rise delay of a fuel from its cetane number and from the relevant parameters of direct-injection diesel engines. *SAE Transactions*, pp.1823-1834. https://doi.org/10.4271/790493

Hardenberg, H.O., and Ehnert, E.R., 1981. Ignition quality determination problems with alternative fuels for compression ignition engines,*SAE Technical Paper*. https://doi.org/10.4271/811212

Heywood, J. B. L.,1988. *Internal combustion engine fundamentals*, McGraw-Hill Inc, USA, ISBN 0-07-028637-X.

Huang, Z., Wang, J., Liu, B., Zeng, K., Yu, J., and Jiang, D.,2007. Combustion characteristics of a direct-injection engine fueled with natural gas hydrogen blends under different ignition timings, 86 (3), pp. 381-387. https://doi.org/10.1016/j.fuel.2006.07.007

Hussain, M., Zaidi, K., and Rehman, S., 2013. Effects of varying injection pressure on ignition delay characteristics of biodiesel, *International Journal of Engineering and Mathematical Sciences*, 3(1), pp. 11 -17.

Hansen, A.C., Zhang, Q., and Lyne, P.W., 2005. Ethanol–diesel fuel blends: a review. *Bioresource Technology*, 96 (3), pp. 277-285. https://doi.org/10.1016/j.biortech.2004.04.007

Ibrahim,J.A.K., Adel, H., AbdAlameer, M.H.,2017. Production of biofuels from selected cellulosic waste materials, *Journal of Engineering*, 23 (8), pp. 46-55. https://doi.org/10.31026/j.eng.2017.08.04

Kwanchareon, P., Luengnaruemitchai, A., Samai J., 2007. Solubility of a diesel–biodiesel–ethanol blend, its fuel properties, and its emission characteristics from diesel engine, *Fuel*, 86 (8), pp.1053-1061. https://doi.org/10.1016/j.fuel.2006.09.034

Kasaby, M., Nemit A. M., 2013. Experimental investigations of ignition delay period and performance of a diesel engine operated with jatropha oil biodiesel, *Alexandia engineering journal*, 52 (2), pp. 141-149. https://doi.org/10.1016/j.aej.2012.12.006

Kwon S., Masataka A., Hiroyasu H., 1989. Effects of cylinder temperature and pressure on ignition delay in direct injection diesel engine, *Translated from Journal of MESJ*, 24 (1), pp. 3-16. https://doi.org/10.5988/JIME1966.24.26

Mustafa, B., Havva, B., Cahide Ö., 2008. Progress in bioethanol processing, *Progress in Energy and Combustion Science*, 34 (5), pp. 551-573. https://doi.org/10.1016/j.pecs.2007.11.001

Navindgi, M., C., Maheswar D., Kumar, B., S., P.,2012. Comparative experimental investigation of combustion, performance and emission in a single cylinder thermal barrier coated diesel engine using diesel and neem biodiesel, *International Journal of Engineering Research and Development*, 3 (2), pp. 12-20. https://doi.org/10.17577/IJERTV2IS60742

Pulkarbed, W.W., 1997. Engineering fundamental of the internal combustion engine. *University of Wisconsin, New Jersey*, pp. 251-270.

Rodriguez, R.P., Sierens, S., Verhelst, S., 2011. Ignition delay in a palm oil and rapeseed oil biodiesel fueled engine and predicate correlation for the ignition delay period, 90, pp. 766-772. https://doi.org/10.1016/j.fuel.2010.10.027

Saadi,T.K., Hassan, A.A., Hussein, A.Y.,2016. Experimental and theoretical study for the effect of diesel fuel quality produced in iraq on ignition delay period, *Eng. &Tech.Journal*, 34 (12), pp. 2258- 2271. https://doi.org/10.30684/etj.34.12A.9.

Sahoo P.K., Das L.M., 2009. Combustion analysis of jatropha, karanja and polanga based biodiesel as fuel in a diesel engine, 88 (6), pp. 994-999. https://doi.org/10.1016/j.fuel.2008.11.012

Sahoo, P.K., Naik,S.N., Das L. M.,2005. Studies on biodiesel production technology from jatropha curcas and its performance in a CI engine, *Journal of Agricultural Engineering Indian Society of Agricultural Engineering (ISAE)*, 42 (2), pp. 18–24.

Selvakumar, R., Nithiyananadam, T., Senthilkumar, P., 2015. A theoretical model to predict the ignition delay and its effects on performance and emission characteristics of biodiesel fueled diesel engine.*Journal of Chemical and Pharmaceutical Sciences, JCHPS Special,*(6), pp.19-23.

Shahabuddin, M., Liaquat, M., Masjuki, H., H., Kalam, M .A. , Mofijur , M . ,2013. Ignition delay, combustion and emission characteristics of diesel engine fueled with biodiesel, *Renewable and Sustainable Energy Reviews*, 21, pp. 623–632. https://doi.org/10.1016/j.rser.2013.01.019

Shahrani, A. S.,2017. Theoretical analysis of ignition in diesel engines, *Journal of Power and Energy Engineering*, 5 (6), pp. 1-13. https://doi.org/.4236/jpee.2017.56001

Soner Gumus, Hakan Ozcan, Mustafa Ozbey, Bahattin Topaloglu, 2016. Aluminum oxide and copper oxide nanodiesel fuel properties and usage in a compression ignition engine. *Fuel*, 163, pp. 80-87. https://doi.org/10.1016/j.fuel.2015.09.048

Stringer, E. W., Clarke, A. E., Clarke, J., S., 1970. The sidpontaneous ignition of hydro carbon fuels in a flowing system, *Proceedings of the Institution of Mechanical Engineers Conference Proceedings*, 184 (10). https://doi.org/10.1243/PIME_CONF_1969_184_334_02

Taylor, C.F., 1985. *The internal combustion engine in theory and practice*. 2nd ed. The MIT Press. https://doi.org/10.7551/mitpress/3851.001.0001

Teng, H., James, C., McCandless, Jeffrey, B., Schneyer, 2003. Compression ignition delay (physical and chemical) of dimethyl ether, an alternative fuel for compression-ignition engines, *Engineering, Chemistry, SAE Technical Paper*, pp. 1-15. https://doi.org/10.4271/2003-01-0759

Watson, N., Pilley, A., Marzouk, M., 1980. A combustion correlation for diesel engine simulation. *SAE Technical paper*. https://doi.org/10.4271/800029

Wolfer, H.H.,1938. Ignition lag in diesel engines. *VDI-Forschungsheft*, 39 (2), pp. 621-647.

Yahuza, I., Dandakouta, H.,2015. A performance review of ethanol-diesel blended fuel samples in compression-ignition engine, *Chemical Engineering & Process Technology*, 6 (5), pp 2-6. https://doi.org/10.4172/2157-7048.1000256

Wrage, K.E., Goering, C.E., 1980. Technical feasibility of diesel, *Transactions of the ASAE*, 23(6), pp. 1338-1343. https://doi.org/10.13031/2013.34775

Zheng, J.J., Wang, J.H., Wang, B., Huang, Z.H.,2009. Effect of the compression ratio on the performance and combustion of a natural-gas direct-injection engine. *Journal of Automobile Engineering,* 223 (1). https://doi.org/10.1243/09544070JAUTO976

APPENDIX

Appendix A: Stochastic A/F computation for each blend of diesel fuel.

For **E0**

$C_{16}H_{32} + 24(O_2 + 3.76N_2) \rightarrow 16CO_2 + 16H_2O + 90.24N_2$

$$\gg\gg (\frac{A}{F})_{Stoich} = 14.74 \frac{kg\ air}{kg\ \ fuel}$$

For **E5**

$0.95C_{16}H_{32} + 0.05(C_2H_5OH) + 22.95(O_2 + 3.76N_2) \rightarrow 15.3\ CO_2 + 15.35\ H_2O + 86.292N_2$

$$\gg\gg (\frac{A}{F})_{Stoich} = 14.68 \frac{kg\ air}{kg\ \ fuel}$$

For **E10**

$0.9C_{16}H_{32} + 0.1(C_2H_5OH) + 21.9(O_2 + 3.76N_2) \rightarrow 14.6\ CO_2 + 14.7\ H_2O + 82.344N_2 \quad \gg$

$$\gg (\frac{A}{F})_{Stoich} = 14.61 \frac{kg\ air}{kg\ \ fuel}$$

For **E15**

$0.85C_{16}H_{32} + 0.15(C_2H_5OH) + 20.85(O_2 + 3.76N_2) \rightarrow 13.9\ CO_2 + 14.05\ H_2O + 78.396N_2$

$$\gg\gg (\frac{A}{F})_{Stoich} = 14.54 \frac{kg\ air}{kg\ \ fuel}$$

For **E20**

$0.8\ C_{16}H_{32} + 0.2(C_2H_5OH) + 19.8\ (O_2 + 3.76N_2) \rightarrow 13.2\ CO_2 + 13.4\ H_2O + 74.448\ N_2$

$$\gg\gg (\frac{A}{F})_{Stoich} = 14.46 \frac{kg\ air}{kg\ \ fuel}$$

توقع فترة تأخير الاشتعال في محركات الاشتعال بالانضغاط باستخدام خلائط إيثانول/ديزل

هيمن عثمان غريب[1*]، حسن عبدالوهاب انجل[2]

[1]قسم الهندسة الميكانيكية والميكاترونيكس، كلية الهندسة، جامعة صلاح الدين، أربيل، العراق
[2]قسم الهندسة الجوية، كلية الهندسة الفنية، جامعة الكتاب، كركوك، العراق

الخلاصة

سمة رئيسية للمحركات الديزل هي القدرة على توقع فترة تأخير الاشتعال. تتنبأ هذه الدراسة بفترة تأخير الاشتعال في محركات الديزل باستخدام مجموعات من خليط الإيثانول/وقود الديزل وكذلك الديزل النقي كبديل للوقود. الهدف الرئيسي لهذا العمل هو توفير صيغ تجريبية لتوقع فترات التأخير. تدفع هذه الدراسة الاهتمام المتزايد بالمزيج من الوقود البديل، الذي يمثل تحولاً كبيرا عن استخدام الوقود الديزل التقليدي. يركز الدراسة الحديثة على فحص هذه المزيجات وكيف يمكن أن تؤثر على ديناميات الاحتراق في محركات الديزل. تم إجراء التجارب باستخدام خمسة خلائط مختلفة من الإيثانول/وقود الديزل، بما في ذلك الديزل النقي، مع تغيير نسب الإيثانول من 5% إلى 20% بنسب قدرها 5%. تم إجراء الاختبارات بسرعة ثابتة للمحرك تبلغ 1500 دورة في الدقيقة، مع نسب ضغط مختلفة تبلغ 16 و17 و18، مع مستويات عزم الدوران تتراوح من 0 إلى 21 نيوتن متر. في هذه الدراسة، تم بناء صيغ عامة لتوقع فترة التأخير الاشتعالي عددياً. كان هناك درجة أكبر من التوافق بين النتائج التجريبية وتوقعات تأخير الاشتعال. أظهرت النتائج أنه عبر جميع متغيرات نسب الضغط، كان خليط الوقود E20 المدمج يظهر بشكل مستمر أقل فترة تأخير اشتعالي. علاوة على ذلك، أظهرت نتائج الاستقصاءات أن فترة تأخير الاشتعال تبدأ في الانخفاض مع زيادة رقم السيتان، وضغط الاشتعال، ودرجة الحرارة، ونسبة المكافئة. تعتبر فترة تأخير الاشتعال الأقصر نتيجة زيادة نسب الضغط. النموذج التنبؤي الذي تم إنشاؤه هنا هو إضافة مبتكرة للصناعة، مما يقدم أساسا قويا لتقييم كفاءة وخصائص الانبعاثات لمختلف خلائط الإيثانول/الديزل.

الكلمات المفتاحية: فترة تأخير الاشتعال، إيثانول، نسبة المكافئ، رقم السيتان